



Synthesis, characterization, and ethylene polymerization behavior of Cr(III) catalysts based on bis(pyrazolylmethyl)pyridine and its derivatives



Jeong Oh Woo, Sung Kwon Kang, Jong-Eun Park, Kyung-sun Son*

Department of Chemistry, Chungnam National University, Daejeon 305-764, Republic of Korea

ARTICLE INFO

Article history:

Received 12 January 2015

Received in revised form 9 April 2015

Accepted 13 April 2015

Available online 14 April 2015

Keywords:

Polymerization

Chromium catalyst

Polyethylene

Organometallic catalyst

ABSTRACT

New chromium(III) [Cr(III)] catalysts based on 2,6-bis(pyrazol-1-ylmethyl) pyridine derivatives have been synthesized, characterized, and evaluated for ethylene polymerization. All ligands with substituents on the pyrazole rings were analyzed by single-crystal X-ray diffraction to clearly identify isomer structures. Additionally, X-ray analyses of the new Cr(III) complex bearing 2,6-bis[(4,5-dimethyl-1H-pyrazol-1-yl) methyl]pyridine showed tridentate coordination on the *mer*-octahedral chromium sphere. Upon activation with dry methaluminumoxane, the precatalysts produce polyethylene (PE) as a major product, and their catalytic performances were affected by the substituents on the pyrazole units; the introduction of functional groups on the pyrazole raised PE compositions and the molecular weight of the PE.

© 2015 Elsevier B.V. All rights reserved.

1. Introduction

The development of homogeneous chromium (Cr)-based catalysts for olefin polymerization has received considerable attention, spurred by the extensive use of Cr catalysts in commercial ethylene polymerization [1,2]. At the interface of late transition metal and early metal metallocene catalysts, Cr has been used in various polymerization studies using a variety of ligands possessing homo- and heteroatom donor sets [3–7]. Since the discovery of Brookhart [8,9] and Gibson-type [10,11] catalysts, new catalyst families of tridentate nitrogen-based ligands such as 2,6-bis(imino) pyridine increased interest in the design of further non-metallocene olefin polymerization catalysts [12–18].

Another interesting, but less explored, type of tridentate nitrogen-based ligands in olefin polymerization is tris(pyrazolyl) borate [19] or tris(pyrazolyl) methane [20,21], in which the coordination chemistry has been studied extensively, but not in terms of olefin polymerization [22–31]. One of the benefits regarding the pyrazolyl unit is the possibility of modifying the architecture of the ligands due to the three possible substituting positions on the pyrazole ring, permitting tuning of the electronic and steric properties depending on the substituents used, offering great possibilities in modifying catalytic behavior.

As an extension of this idea, we chose the combination of pyridyl and pyrazolyl units with various substituents to search for new polymerization catalysts and to further investigate ligand structures in catalytic performance [32]. In this report, we present the synthesis and characterization of ethylene polymerization catalysts based on Cr(III) with 2,6-bis(pyrazol-1-ylmethyl) pyridine derivatives [33–35], as well as their catalytic behavior toward ethylene polymerization. The molecular structures of the new ligands were determined by single-crystal X-ray diffraction to confirm unambiguously the structures of the isomers. To better understand the molecular structures of the Cr(III) precatalysts, their single crystals were also obtained and analyzed structurally.

2. Experimental

2.1. General considerations

All manipulations were carried out under a nitrogen atmosphere using standard Schlenk techniques or in a purified nitrogen-filled dry box, unless otherwise stated. Methylaluminoxane (MAO, 10% in toluene) was purchased from Albemarle Corporation (Baton Rouge, LA, USA). Trimethyl aluminum (TMA)-free dry methylaluminoxane (dMAO) was prepared by removing all volatiles from MAO *in vacuo*. Pyrazole, 3-phenyl-1H-pyrazole, 3-tert-butyl-1H-pyrazole, *p*-toluenesulfonyl chloride, 2,6-pyridinedimethanol, CrCl₃(THF)₃, and Cr(acac)₃ were purchased from Sigma–Aldrich (St. Louis, MO, USA). 3,4-Dimethyl-1H-pyrazole, 3-trifluoromethyl-1H-

* Corresponding author. Tel.: +82 0 42 821 6547.
E-mail address: kson@cnu.ac.kr (K.-s. Son).

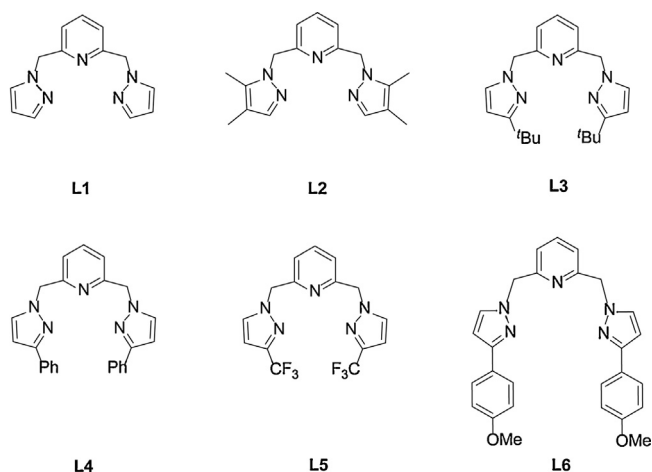


Fig. 1. Structures of the ligands **L1**–**L6**.

pyrazole, and 3-(4-methoxyphenyl)-1H-pyrazole were purchased from Alfa Aesar (Ward Hill, MA, USA).

All solvents were dried and distilled prior to use according to standard methods. For instance, toluene was refluxed over sodium/benzophenone until the purple color appeared and distilled under nitrogen prior to use. All other chemical reagents were purchased from commercial sources and used as received unless stated otherwise.

^1H and ^{13}C NMR spectra of the ligand products were recorded at 25°C on a Fourier 300 NMR spectrometer (Bruker, Billerica, MA, USA) with tetramethylsilane (TMS) as an internal reference. ^{13}C NMR spectra of the polyethylene (PE) samples were recorded on a Bruker Avance III 600 at 130°C in a 50:50 v/v solution of 1,2-dichlorobenzene/1,2-dichlorobenzene- d_4 in the presence of Cr(III) acetylacetonate (1 mM) to reduce the relaxation time of the aliphatic carbons. The oligomers (liquid products) were analyzed by gas chromatography–mass spectrometry (GC–MS) on a Clarus 600 with an Elit-5 (30 m \times 0.25 mm \times 0.25 μm column; PerkinElmer, Waltham, MA, USA) using nonane as an internal standard. Molecular weights and polydispersity indices (PDIs) of PE were determined by high-temperature gel permeation chromatography (GPC) on a PL-GPC 220 instrument with a refractive index (RI) detector (Agilent, Santa Clara, CA, USA), calibrated with polystyrene standards at 160°C and 1,2,4-trichlorobenzene as the eluent. Melting points of the polymer were determined by differential scanning calorimetry (DSC) with a DSC-1 instrument (Mettler-Toledo, Columbus, OH, USA) in standard DSC run mode. The instrument was initially calibrated for the melting point of an indium standard. The polymer sample was first heated to 160°C to remove thermal history, and a second heating cycle was used for collecting DSC thermogram data at a ramping rate of 5°C min^{-1} . Elemental analysis was performed on a Flash EA 1112 automatic elemental analyzer (Thermo Fisher Scientific, Waltham, MA, USA). X-ray crystal data were obtained using a SMART APEX II (Bruker) single crystal X-ray diffractometer equipped with a Bruker SMART charge-coupled device (CCD) area detector. The Fourier-transform infrared (FTIR) spectrum was recorded with an FTIR 4100 spectrometer (JASCO, Tokyo, Japan). Mass spectra were recorded on a JEOL JMS-600W (EI) spectrometer or a Bruker micrOTOF-QII (ESI) spectrometer.

2.2. Synthesis of ligands

2.2.1. Preparation of 2,6-pyridine-dimethylene-ditosylate

At 0°C , a solution of *p*-toluenesulfonyl chloride (0.76 g, 4.0 mmol) in tetrahydrofuran (THF; 7.5 mL) was added to a stirred solution of 2,6-pyridinedimethanol (0.28 g, 2.0 mmol) and NaOH

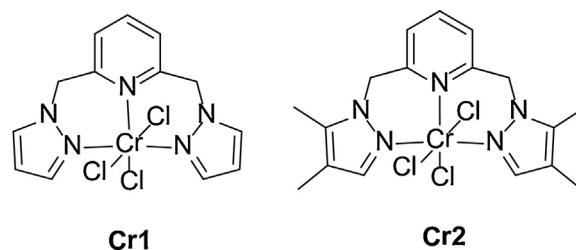


Fig. 2. Structures of Cr(III) complexes **Cr1** and **Cr2**.

(0.8 g, 20 mmol) in THF/water (7.5/7.5 mL). After 4 h of stirring, the mixture was poured into 20 mL of water and extracted with methylene chloride (3×7.5 mL). The organic phase was washed with saturated aqueous NaCl solution and distilled water and dried over Na_2SO_4 ; the solvent was removed *in vacuo* to afford 2,6-pyridine-dimethylene-ditosylate (0.79 g, 88%) as a white powder. ^1H NMR (300 MHz, CDCl_3): δ = 7.80 (d, J = 7.5 Hz, 4H, 2,6-*H* tosyl), 7.69 (t, J = 7.5 Hz, 1H, 4-*H* Py), 7.32 (d, 2H, 3,5-*H* Py, d, 4H, 3,5-*H* tosyl), 5.04 (s, 4H, PyCH_2 tosyl), and 2.44 (s, 6H, tosyl- CH_3) Fig. 1.

2.2.2. Preparation of 2,6-bis[(pyrazol-1-yl) methyl]pyridine (**L1**) [33,36–38]

At 0°C , a solution of pyrazole (0.22 g, 3.2 mmol) in dry THF (5 mL) was added dropwise to a suspension of NaH (0.08 g, 3.2 mmol) in dry THF (5 mL). After 15 min of stirring, a clear solution of NaPz was obtained. A solution of 2,6-pyridine-dimethylene-ditosylate (0.73 g, 1.6 mmol) in dry THF (7.5 mL) was added to this solution; the mixture was stirred overnight and filtered, and the solvent was removed. The crude product was purified by column chromatography on silica gel with ethyl acetate (EA) as eluent to afford 0.30 g (76%) of pure ligand as a white solid. ^1H NMR (300 MHz, acetone- d_6): δ 7.77 (d, J = 2.4 Hz, 2H, 5-*H* Pz), 7.66 (t, J = 7.8 Hz, 1H, 4-*H* Py), 7.48 (d, J = 1.5 Hz, 2H, 3-*H* Pz), 6.83 (d, J = 7.8 Hz, 2H, 3,5-*H* Py), 6.30 (t, J = 2.1 Hz, 2H, 4-*H* Pz), and 5.44 (s, 4H, PyCH_2Pz). ^{13}C NMR (75 MHz, acetone- d_6): δ 157.9 (2C, 2,6-*C* Py), 140.1 (2C, 3-*C* Pz), 138.6 (2C, 5-*C* Pz), 131.0 (1C, 4-*C* Py), 120.9 (2C, 3,5-*C* Py), 106.4 (2C, 4-*C* Pz), 57.7 (2C, PyCH_2Pz).

2.2.3. Preparation of 2,6-bis[(4,5-dimethyl-1H-pyrazol-1-yl) methyl]pyridine (**L2**)

At 0°C , a solution of 3,4-dimethyl-1H-pyrazole (1.66 g, 17.3 mmol) in dry THF (30 mL) was added dropwise to a suspension of NaH (0.41 g, 17.3 mmol) in dry THF (30 mL). After 15 min of stirring, a solution of 2,6-pyridine-dimethylene-ditosylate (3.87 g, 8.64 mmol) in dry THF (45 mL) was added to this solution; the mixture was stirred overnight and filtered, and the solvent was removed. The crude product was purified by column chromatography on silica gel with EA as eluent to afford 1.63 g (64%) of pure ligand as a white solid. Single crystals were obtained by slow diffusion of hexane into a concentrated solution of the ligand in THF at room temperature. ^1H NMR (300 MHz, acetone- d_6): δ 7.63 (t, J = 7.8 Hz, 1H, 4-*H* Py), 7.19 (s, 2H, 3-*H* Pz), 6.72 (d, J = 7.8 Hz, 2H, 3,5-*H* Py), 5.31 (s, 4H, PyCH_2Pz), 2.14 (s, 6H, Pz-5-*Me*), and 1.97 (s, 6H, Pz-4-*Me*). ^{13}C NMR (75 MHz, acetone- d_6): δ 158.3 (2C, 2,6-*C* Py), 139.6 (2C, 3-*C* Pz), 138.6 (2C, 5-*C* Pz), 136.4 (1C, 4-*C* Py), 120.6 (2C, 3,5-*C* Py), 114.0 (2C, 4-*C* Pz), 55.4 (2C, PyCH_2Pz), 9.18 (2C, Pz-5-*Me*), and 8.79 (2C, Pz-4-*Me*). HRMS (ESI) Calcd for $\text{C}_{17}\text{H}_{21}\text{N}_5\text{Na}$ ($[\text{M}+\text{Na}]^+$): 318.1695, Found: 318.1709.

2.2.4. Preparation of 2,6-bis[(3-(tert-butyl)-1H-pyrazol-1-yl) methyl]pyridine (**L3**)

At 0°C , a solution of 3-tert-butyl-1H-pyrazole (0.05 g, 0.40 mmol) in dry THF (1 mL) was added dropwise to a suspension of NaH (0.01 g, 0.40 mmol) in dry THF (1 mL). After 15 min

of stirring, a solution of 2,6-pyridine-dimethylene-ditosylate (0.09 g, 0.20 mmol) in dry THF (1.5 mL) was added to this solution; the mixture was stirred overnight and filtered, and the solvent was removed. The crude product was purified by column chromatography on silica gel with EA as eluent to afford 0.05 g (72%) of pure ligand as a white solid. Single crystals were obtained by slow diffusion of hexane into a concentrated solution of the ligand in THF at room temperature. $^1\text{H NMR}$ (300 MHz, acetone- d_6): δ 7.64 (t, J = 7.8 Hz, 1H, 4-*H* Py), 7.61 (d, J = 2.4 Hz, 2H, 5-*H* Pz), 6.79 (d, J = 7.8 Hz, 2H, 3,5-*H* Py), 6.17 (d, J = 2.4 Hz, 2H, 4-*H* Pz), 5.36 (s, 4H, PyCH_2Pz), and 1.27 (s, 18H, $t\text{Bu}$). $^{13}\text{C NMR}$ (75 MHz, acetone- d_6): δ 162.6 (2C, 3-*C* Pz), 158.3 (2C, 2,6-*C* Py), 138.6 (1C, 4-*C* Py), 131.4 (2C, 5-*C* Pz), 120.7 (2C, 3,5-*C* Py), 102.6 (2C, 4-*C* Pz), 57.6 (2C, PyCH_2Pz), 32.7 (2C, $\text{C}(\text{CH}_3)_3$), and 31.0 (6C, $\text{C}(\text{CH}_3)_3$). HRMS (EI) Calcd for $\text{C}_{21}\text{H}_{29}\text{N}_5$ (M^+): 351.2423, Found: 351.2417.

2.2.5. Preparation of 2,6-bis[(3-phenyl-1H-pyrazol-1-yl)methyl]pyridine (**L4**) [39,40]

At 0 °C, a solution of 3-phenyl-1H-pyrazole (0.61 g, 5.3 mmol) in dry THF (10 mL) was added dropwise to a suspension of NaH (0.13 g, 5.34 mmol) in dry THF (10 mL). After 15 min of stirring, a solution of 2,6-pyridine-dimethylene-ditosylate (1.20 g, 2.67 mmol) in dry THF (15 mL) was added to this solution; the mixture was stirred overnight and filtered, and the solvent was removed. The crude product was purified by column chromatography on silica gel with hexane:EA = 1:1 as eluent to afford 0.41 g (40%) of pure ligand as a white oil that solidified with time. Single crystals were obtained by slow diffusion of hexane into a concentrated solution of the ligand in THF at room temperature. $^1\text{H NMR}$ (300 MHz, acetone- d_6): δ 7.84 (m, 2H, 4H, 5-*H* Pz, 2,6-*H* Ph), 7.65 (t, J = 7.8 Hz, 1H, 4-*H* Py), 7.36 (t, J = 7.2 Hz, 4H, 3,5-*H* Ph), 7.26 (t, J = 7.5 Hz, 2H, 4-*H* Ph), 6.96 (d, J = 7.8 Hz, 2H, 3,5-*H* Py), 6.72 (d, J = 2.4 Hz, 2H, 4-*H* Pz), and 5.48 (s, 4H, PyCH_2Pz). $^{13}\text{C NMR}$ (75 MHz, acetone- d_6): δ 157.9 (2C, 2,6-*C* Py), 152.2 (2C, 3-*C* Pz), 138.9 (1C, 4-*C* Py), 134.8 (2C, 1-*C* Ph), 132.9 (2C, 5-*C* Pz), 129.3 (4C, 3,5-*C* Ph), 128.2 (2C, 4-*C* Ph), 126.1 (4C, 2,6-*C* Ph), 121.2 (2C, 3,5-*C* Py), 103.7 (2C, 4-*C* Pz), and 57.9 (2C, PyCH_2Pz).

2.2.6. Preparation of 2,6-bis[(3-(trifluoromethyl)-1H-pyrazol-1-yl)methyl]pyridine (**L5**)

At 0 °C, a solution of 3-trifluoromethyl-1H-pyrazole (0.84 g, 6.20 mmol) in dry THF (10 mL) was added dropwise to a suspension of NaH (0.15 g, 6.20 mmol) in dry THF (10 mL). After 15 min of stirring, a solution of 2,6-pyridine-dimethylene-ditosylate (1.39 g, 3.10 mmol) in dry THF (15 mL) was added to this solution; the mixture was stirred overnight and filtered, and the solvent was removed. The crude product was purified by column chromatography on silica gel with EA as eluent to afford 0.53 g (46%) of pure ligand as a white solid. Single crystals were obtained by slow diffusion of hexane into a concentrated solution of the ligand in THF at room temperature. $^1\text{H NMR}$ (300 MHz, acetone- d_6): δ 7.97 (d, J = 1.5 Hz, 2H, 5-*H* Pz), 7.81 (t, J = 7.8 Hz, 1H, 4-*H* Py), 7.15 (d, J = 7.5 Hz, 2H, 3,5-*H* Py), 6.69 (d, J = 2.4 Hz, 2H, 4-*H* Pz), and 5.55 (s, 4H, PyCH_2Pz). $^{13}\text{C NMR}$ (75 MHz, acetone- d_6): δ 156.7 (2C, 2,6-*C* Py), 142.8 (2C, 3-*C* Pz), 139.2 (1C, 4-*C* Py), 133.6 (2C, 5-*C* Pz), 122.7 (2C, CF_3), 122.0 (2C, 3,5-*C* Py), 105.2 (2C, 4-*C* Pz), and 58.3 (2C, PyCH_2Pz). $^{19}\text{F NMR}$ (564 MHz, acetone- d_6): δ 62.19 (CF_3). HRMS (ESI) Calcd for $\text{C}_{15}\text{H}_{11}\text{F}_6\text{N}_5\text{Na}$ ($[\text{M}+\text{Na}]^+$): 398.0816, Found: 398.0812.

2.2.7. Preparation of 2,6-bis[(3-(4-methoxyphenyl)-1H-pyrazol-1-yl)methyl]pyridine (**L6**)

At 0 °C, a solution of 3-(4-methoxyphenyl)-1H-pyrazole (0.59 g, 3.42 mmol) in dry THF (5 mL) was added dropwise to a suspension of NaH (0.08 g, 3.42 mmol) in dry THF (5 mL). After 15 min of stirring, a solution of 2,6-pyridine-dimethylene-ditosylate (0.77 g,

1.71 mmol) in dry THF (7.5 mL) was added to this solution; the mixture was stirred overnight and filtered, and the solvent was removed. The crude product was purified by column chromatography on silica gel with hexane:EA = 1:1 as eluent to afford 0.40 g (51%) of pure ligand as a white solid. Single crystals were obtained by slow diffusion of hexane into a concentrated solution of the ligand in THF at room temperature. $^1\text{H NMR}$ (300 MHz, acetone- d_6): δ 7.81 (d, J = 2.1 Hz, 2H, 5-*H* Pz), 7.77 (d, J = 9.0 Hz, 4H, 2,6-*H* Ph), 7.70 (t, J = 7.8 Hz, 1H, 4-*H* Py), 6.96 (t, J = 7.2 Hz, 4H, 3,5-*H* Ph), 6.65 (d, J = 2.4 Hz, 2H, 4-*H* Pz), 5.47 (s, 4H, PyCH_2Pz), and 3.81 (s, 6H, PhOCH_3). $^{13}\text{C NMR}$ (75 MHz, acetone- d_6): δ 160.3 (2C, 4-*C* Ph), 158.1 (2C, 2,6-*C* Py), 152.2 (2C, 3-*C* Pz), 138.8 (1C, 4-*C* Py), 132.8 (2C, 5-*C* Pz), 127.5 (2C, 1-*C* Ph), 127.4 (4C, 2,6-*C* Ph), 121.2 (2C, 3,5-*C* Py), 114.7 (4C, 3,5-*C* Ph), 103.1 (2C, 4-*C* Pz), 57.9 (2C, PyCH_2Pz), and 55.6 (2C, PhOCH_3). HRMS (EI) Calcd for $\text{C}_{27}\text{H}_{25}\text{N}_5\text{O}_2$ (M^+): 451.2008, Found: 451.2008.

2.3. Synthesis of LCrCl_3

Cr complexes were synthesized by the reaction of $\text{CrCl}_3(\text{THF})_3$ with the corresponding ligands in THF. A typical synthetic procedure was as follows Fig. 2.

2.3.1. Synthesis of trichloro[2,6-bis[(pyrazol-1-yl)methyl]pyridine]chromium(III) (**Cr1**)

L1 (0.072 g, 0.3 mmol) in dry THF (4 mL) was added to a solution of $\text{CrCl}_3(\text{THF})_3$ (0.112 g, 0.3 mmol) in dry THF (6 mL); the resulting mixture was stirred at 60 °C for 24 h, giving a green suspension. After the solvent was removed, the product was washed repeatedly with THF and diethyl ether, and dried *in vacuo*. The green powder (0.091 g) was obtained in a yield of 76%. Calc. for $\text{C}_{13}\text{H}_{13}\text{Cl}_3\text{CrN}_5$: C, 39.27; H, 3.30; N, 17.61. Found: C, 39.21; H, 3.34; N, 17.45%.

2.3.2. Synthesis of trichloro[2,6-bis[(4,5-dimethyl-1H-pyrazol-1-yl)methyl]pyridine]chromium(III) (**Cr2**)

The complex **Cr2** was prepared as a green powder by a similar procedure in a yield of 79%. Single crystals were obtained by slow diffusion of diethyl ether into a concentrated solution of the complex in dimethyl sulfoxide (DMSO) at room temperature. Calc. for $\text{C}_{17}\text{H}_{21}\text{Cl}_3\text{CrN}_5$: C, 45.00; H, 4.66; N, 15.43. Found: C, 45.02; H, 4.77; N, 15.47%.

2.4. General procedure for ethylene polymerization

These reactions were carried out in a 125 mL Parr reactor equipped with a pressure controller. The desired amounts of dMAO (0.174 g, 3 mmol, 300 eq) and dry toluene (46 mL) were added to the reactor. After the desired reaction temperature was achieved (45 °C), the reactor was charged with ethylene at a constant pressure (10 bar), and (i) a toluene solution (4 mL) of $\text{Cr}(\text{acac})_3$ (3.5 mg, 0.01 mmol) and NNN ligand (0.02 mmol) or (ii) a toluene solution (4 mL) of Cr complex (0.01 mmol) was injected into the reactor to start the reaction. After 15 min, the reaction was terminated by discontinuing the ethylene feed and adding methanol (10 mL) to the reactor. Then, the reactor was cooled to below 5 °C in an ice bath. After releasing the excess ethylene from the reactor, nonane (1 mL) was added as an internal standard for the GC–MS analysis of the liquid phase. A small amount of the reaction solution was collected and analyzed by GC–MS to determine the distribution of oligomers obtained. The remainder of the mixture was quenched with methanol/HCl (10 vol%) to precipitate the solid product, which was isolated by filtration, dried in a vacuum oven at 60 °C, and finally characterized by GPC and DSC.

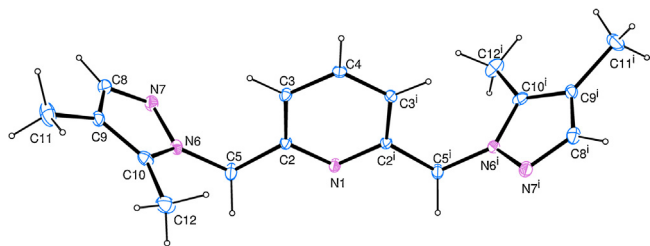


Fig. 3. Thermal ellipsoid representation (25% probability boundaries) of the molecular structure of **L2** [symmetry code: (i) $-x+1, y, -z+3/2$].

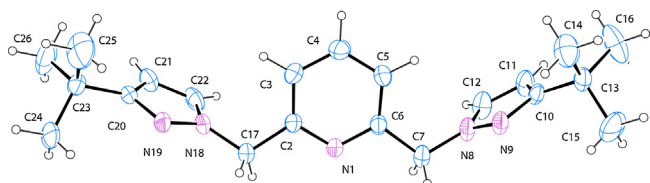


Fig. 4. Thermal ellipsoid representation (25% probability boundaries) of the molecular structure of **L3**.

3. Results and discussion

3.1. Preparation and characterization of **L1–L6** and **Cr1–Cr2**

The new ligands derived from 2,6-bis(pyrazol-1-ylmethyl)pyridine (**L1–L6**) were prepared as described previously (Scheme 1) [33], starting from substituted pyrazole salt with 2,6-pyridinedimethanol. All tridentate ligands were characterized by ^1H and ^{13}C NMR spectroscopy. Additionally, ligands **L2–L6** were further characterized by X-ray crystallography to confirm unambiguously the structures of the isomers. Suitable single crystals were obtained from slow diffusion of *n*-hexane into a concentrated solution of the ligand in THF at room temperature. Perspective views of the molecules are shown in Figs. 3–7, and bond distances and angles are included in Tables S1–S10. The pyrazole groups connected to the methylene spacers were placed on opposite sides of the pyridine plane, and all bond distances and bond angles fell within expected ranges. The substituents were located at the 3-position of the pyrazole rings in **L3–L6**, whereas the methyl groups in **L2** were found at the 4,5-positions.

To better understand the molecular structures of the Cr(III) precatalysts, we tried to prepare and obtain suitable single crystals. The Cr precatalysts **Cr1** and **Cr2** were formed through the treatment of $\text{CrCl}_3(\text{THF})_3$ with equimolar amounts of **L1** and **L2**, respectively. These complexes were isolated in good yield (>76%) as neutral octahedral complexes. Experimental values of elemental analysis of the

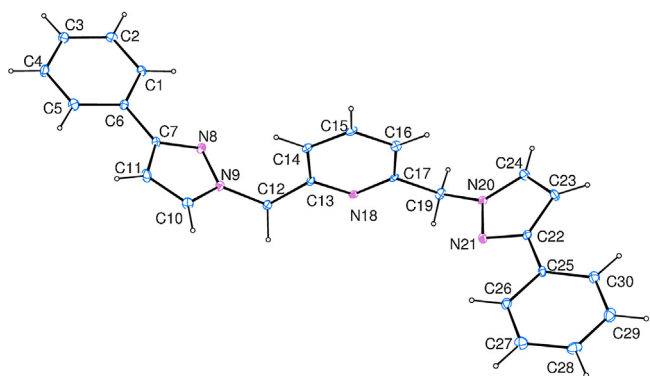


Fig. 5. Thermal ellipsoid representation (25% probability boundaries) of the molecular structure of **L4**.

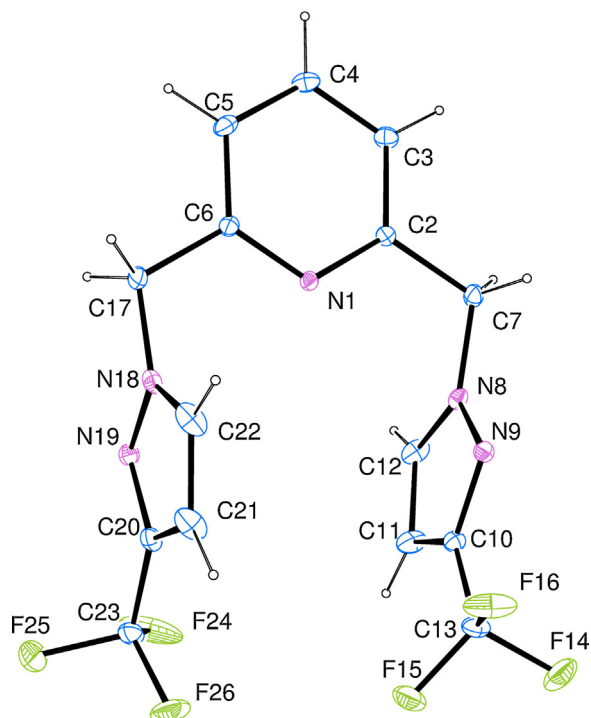


Fig. 6. Thermal ellipsoid representation (25% probability boundaries) of the molecular structure of **L5**.

isolated complexes were consistent with the expected theoretical values, assuming the general formula LCrCl_3 . They are powder-like and exhibit low solubility in common organic solvents, excluding DMSO. The solubility of Cr complexes in DMSO allowed us to obtain single crystals of **Cr2**, which were analyzed by X-ray crystallography to determine structural information. The crystal was obtained from a slow diffusion of diethyl ether into a solution of DMSO at room temperature. The compound has a monoclinic crystalline system and its molecular structure is shown in Fig. 8. This is the first crystal structure determined by X-ray crystallography of a Cr(III) complex bearing 2,6-bis(pyrazol-1-ylmethyl)pyridine. As shown in Fig. 8, solid-state structure of **Cr2** revealed that coordination sphere of the Cr center adopts an octahedral geometry with a tridentate ligand and three chlorines. In the molecular structure of **Cr2**, the donor nitrogen atoms form a *mer* configuration; the basal plane consists of the three nitrogen atoms from the pyridine and pyrazoles and one equatorial chloride, with the remaining chlorides occupying the apical positions [37]. The structure can be compared to that of 2,6-bis(2-benzimidazolyl)pyridine Cr(III) complex reported by Zhang et al. [16]. Similarities include the fact that the bond lengths between the Cr and the mutually *trans*-disposed chlorine atoms, Cr1–Cl2 and Cr1–Cl2ⁱ (2.3329(16) Å), are longer than the bond length of Cr1–Cl3 (2.303(2) Å). However, the Cr–N(pyridine)

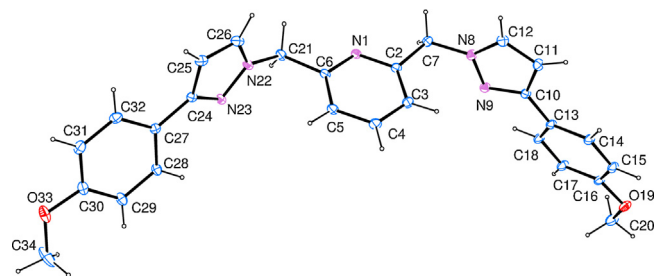


Fig. 7. Thermal ellipsoid representation (25% probability boundaries) of the molecular structure of **L6**.

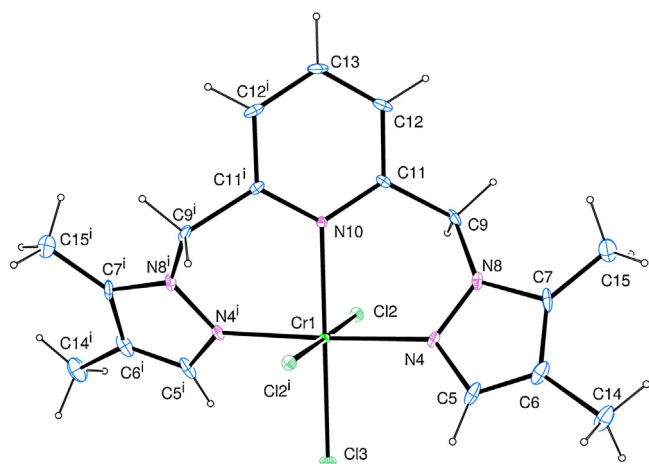


Fig. 8. Thermal ellipsoid representation (25% probability boundaries) of the molecular structure of **Cr2** [symmetry code: (i) $-x+1, y, -z+1/2$].

bond distance [Cr1–N10 = 2.132(6) Å] is about 0.079 Å longer than the Cr–N(pyrazole) bond distances [Cr1–N4 and Cr1–N4ⁱ = 2.053(5) Å], in contrast to some other Cr complexes [14,16,17], probably due to steric influences. All bond angles in the equatorial plane are very close to a right angle [N4–Cr1–N10 and N4ⁱ–Cr1–N10, 88.85(16)°; N4–Cr1–Cl3 and N4ⁱ–Cr1–Cl3, 91.15(16)°] (Tables S11–S12).

The IR spectra of ligands **L1** and **L2** show that the C=N stretching frequency of pyridine appears at 1594 cm⁻¹ (Figs. S13, S15). In complexes **Cr1** and **Cr2**, the C=N stretching vibrations shift to 1609 cm⁻¹ (Figs. S14, S16), indicating effective coordination between the metal and the nitrogen atom of the pyridine ring.

3.2. Effects of the ligand structure on *in situ* ethylene polymerization

Ligands **L1–L6** and Cr(acac)₃ were reacted *in situ* and tested for ethylene polymerization; the results are summarized in Table 1. In all experiments, the *in situ* complexes were activated with excess dMAO at 45 °C in toluene to generate the active species. Regardless of the type of substituents, they converted ethylene to linear polyethylene with moderate activities (85–140 kg molCr⁻¹ h⁻¹) depending on the ligand environment. Analysis of the data indicated that the substitution of hydrogen on the pyrazole rings (entry 1 vs. entries 2–6) greatly affected the product distribution, leading to increases in PE compositions (%) and in the molecular weights of PE, as determined by GPC measurements and deduced by the melting points (*T*_m). This could have been due to steric hindrance arising around the central Cr by the substituted bis(pyrazolylmethyl) pyridine ligands, resulting in a reduction of the rate of β-H transfer, giving the higher molecular weight PE. Note that the presence of substituents at the 3-position of the pyrazole rings afforded longer PE. For example, entries 3–6 employing **L3–L6** with a substituent at the 3-position generated higher molecular weight PE than **L2** (entry 2), which has a hydrogen at the 3-position of the pyrazoles. The effect of steric factors around

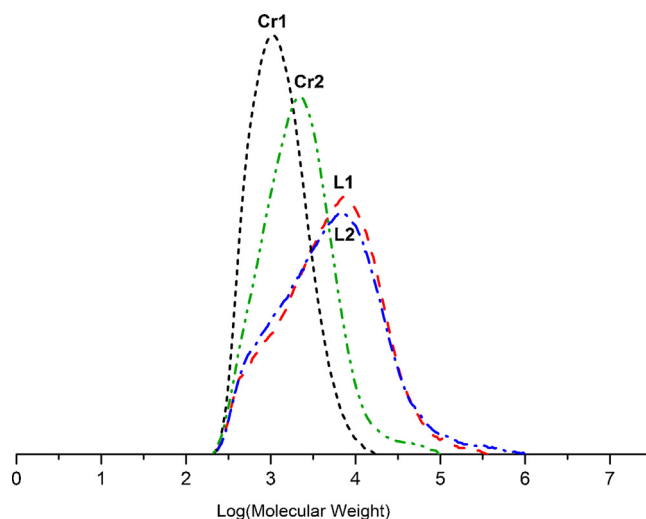


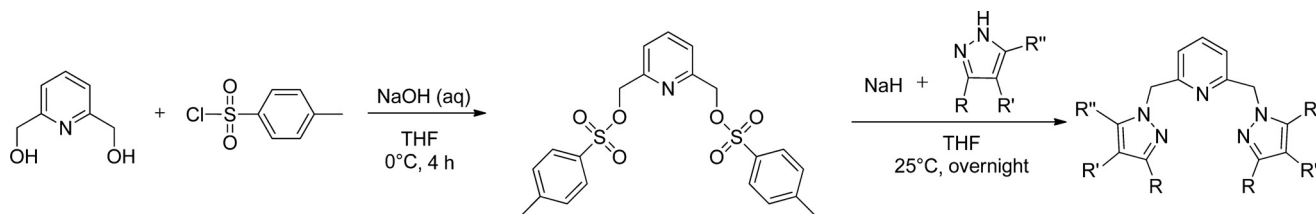
Fig. 9. Gel permeation chromatography (GPC) traces for polyethylene samples obtained from entries 1, 2, 7, and 8 in Tables 1 and 2.

the central metal was also observed in a similar Cr(III) complex bearing 2,6-bis(3,5-dimethylpyrazol-1-ylmethyl) pyridine or 2,6-bis(indazol-2-ylmethyl) pyridine, which was reported to produce high molecular-weight PE of *T*_m 133–135 °C [41]. It is also interesting to compare our results to a previous report with a similar Cr(III) catalyst, such as [2,6-bis(2-benzimidazolyl) pyridyl]chromium chlorides, which has afforded ethylene oligomers and PE with selectivity sensitive to the cocatalysts [15,16]. However, the relationship between the polymerization results and the presence of an electron donating or electron withdrawing group in the pyrazole rings remains unclear.

3.3. Ethylene polymerization with **Cr1** and **Cr2**

The precatalysts **Cr1** and **Cr2** were also activated with excess dMAO in the presence of ethylene. As summarized in Table 2, the complex **Cr2** showed activities twice higher than analog **Cr1** (213 vs. 109 kg molCr⁻¹ h⁻¹). In addition, the substitution of hydrogen on the pyrazole rings resulted in increased PE compositions (%) and molecular weights of PE, consistent with the trends of substituent effects shown in Table 1.

Further comparisons between the *in situ* precatalysts (Table 1) and LCrCl₃ complexes (Table 2) highlight other differences between these Cr systems. GPC analysis of the polymers produced by **Cr1** and **Cr2** exhibited narrower polydispersities (*M*_w/*M*_n = 1.7–2.5) and lower molecular weights (*M*_w = 1633–3528 g mol⁻¹) compared to the *in situ* precatalysts (*M*_w/*M*_n = 5.0–20.0, *M*_w = 10,935–58,874 g mol⁻¹). As shown in Fig. 9, some of the GPC traces of PE exhibited bimodal behavior, which was also observed in the catalytic systems of [2,6-bis(2-benzimidazolyl) pyridyl]chromium chlorides, [16] pyridinebis(imino) chromium chlorides, [14] and [bis(pyridylmethyl) amine]chromium complexes [13]. Based on our results, we propose the presence of two



Scheme 1. Synthesis of 2,6-Bis(pyrazol-1-ylmethyl) pyridine Derivatives.

Table 1
Effects of various ligands (L1–L6) on ethylene polymerization/oligomerization^a

Entry	Ligand	R	R'	R''	Activity ^b	Oligomer distribution (wt%) ^c			PE (wt%)	<i>T</i> _m (°C) ^d	<i>M</i> _w ^e	<i>M</i> _n ^e	PDI ^{e,f}
						1-C ₆ (wt%)	1-C ₈ (wt%)	C ₁₀ –C ₄₀ (wt%)					
1	L1	H	H	H	115	0.10	0.83	13.61	85.46	128.9	10,935	2175	5.0
2	L2	H	Me	Me	87	0.27	0.59	14.14	85.00	128.7	14,611	2096	6.9
3	L3	^t Bu	H	H	140	0.18	2.05	8.20	89.57	130.2	37,659	2452	15.3
4	L4	Ph	H	H	90	0.13	0.84	10.86	88.18	129.2	18,689	2275	8.2
5	L5	CF ₃	H	H	106	0.06	0.22	4.81	94.90	129.9	58,874	2943	20.0
6	L6	MeO-Ph	H	H	85	0.10	0.46	9.13	90.31	129.3	27,423	2249	12.1

^a General reaction conditions: toluene (50 mL), 10 μmol Cr(acac)₃, 20 μmol ligand, 300 equivalent dMAO, 10 bar ethylene, 45 °C, 15 min.

^b In units of kg (mol Cr)⁻¹ h⁻¹.

^c The % yield measured by GC-MS.

^d Determined by DSC.

^e Determined by high-temperature GPC.

^f Polydispersity (PDI) = *M*_w/*M*_n.

Table 2
Ethylene polymerization/oligomerization behavior of Cr1 and Cr2^a.

Entry	Complex	Activity ^b	Oligomer distribution (wt%) ^c			PE (wt%)	<i>T</i> _m (°C) ^d	<i>M</i> _w ^e	<i>M</i> _n ^e	PDI ^{e,f}
			1-C ₆ (wt%)	1-C ₈ (wt%)	C ₁₀ –C ₄₀ (wt%)					
7	Cr1	109	0.46	1.04	38.56	59.93	122.5	1633	950	1.7
8	Cr2	213	0.16	0.95	14.05	84.84	125.8	3528	1378	2.5

^a General reaction conditions: toluene (50 mL), 10 μmol Cr complex, 300 equivalent dMAO, 10 bar ethylene, 45 °C, 15 min.

^b In units of kg (mol Cr)⁻¹ h⁻¹.

^c The % yield measured by GC-MS.

^d Determined by DSC.

^e Determined by high-temperature GPC.

^f Polydispersity (PDI) = *M*_w/*M*_n.

active species in the *in situ* polymerization reaction: one species that is activated from the ligand-binding Cr complex (and also exists during the polymerization with Cr1 and Cr2), while the other is associated with the Cr precursor, Cr(acac)₃.

The NMR spectra demonstrate that all of the PEs are long, linear α-olefins. The ¹³C NMR spectrum of the PE obtained in Fig. S33 demonstrates that the PE sample is highly linear with the presence of end vinyl groups. This is based on the observation of one signal from the methylene groups (–CH₂–) in the ¹³C NMR spectrum, which is evidence of the high linearity of the polymer.

4. Conclusions

In summary, we synthesized and characterized new ligand derivatives of 2,6-bis(pyrazol-1-ylmethyl) pyridine and the octahedral Cr(III) complexes bearing the tridentate ligands in a *mer* configuration, which were shown to be good precatalysts for ethylene polymerization. In the presence of dMAO, these precatalysts exhibited moderate activities (85–213 kg molCr⁻¹ h⁻¹) in ethylene polymerization. The introduction of substituents on the pyrazole rings increased PE compositions (%) and the molecular weights of the PE. The results presented here demonstrate that the catalytic performances are largely affected by the ligand substituents, indicating that rational ligand modifications can lead to predictable product properties. Further studies will focus on increasing our understanding of the relationship between the activity and the electronic effects of the ligands, and studying the influence of the cocatalyst.

Acknowledgments

We gratefully acknowledge financial support from LG Chem and the National Research Foundation of Korea (NRF-2012R1A1A1005839).

Appendix A. Supplementary data

Supplementary data associated with this article can be found, in the online version, at <http://dx.doi.org/10.1016/j.molcata.2015.04.007>.

References

- [1] K.H. Theopold, Eur. J. Inorg. Chem. (1998) 15–24.
- [2] K.M. Smith, Curr. Org. Chem. 10 (2006) 955–963.
- [3] R.D. Kohn, M. Haufe, S. Mihan, D. Lilge, Chem. Commun. (2000) 1927–1928.
- [4] D.J. Jones, V.C. Gibson, S.M. Green, P.J. Maddox, Chem. Commun. (2002) 1038–1039.
- [5] T. Xu, Y. Mu, W. Gao, J. Ni, L. Ye, Y. Tao, J. Am. Chem. Soc. 129 (2007) 2236–2237.
- [6] F. Junges, M.C.A. Kuhn, A.H.D.P. dos Santos, C.R.K. Rabello, C.M. Thomas, J.-F. Carpentier, O.L. Casagrande, Organometallics 26 (2007) 4010–4014.
- [7] J. Al Thagfi, G.G. Lavoie, Organometallics 31 (2012) 2463–2469.
- [8] B.L. Small, M. Brookhart, A.M.A. Bennett, J. Am. Chem. Soc. 120 (1998) 4049–4050.
- [9] B.L. Small, M. Brookhart, J. Am. Chem. Soc. 120 (1998) 7143–7144.
- [10] G.J.P. Britovsek, M. Bruce, V.C. Gibson, B.S. Kimberley, P.J. Maddox, S. Mastroianni, S.J. McTavish, C. Redshaw, G.A. Solan, S. Strömberg, A.J.P. White, D.J. Williams, J. Am. Chem. Soc. 121 (1999) 8728–8740.
- [11] V.C. Gibson, C. Redshaw, G.A. Solan, Chem. Rev. 107 (2007) 1745–1776.
- [12] M.A. Esteruelas, A.M. López, L. Méndez, M. Oliván, E. Oñate, Organometallics 22 (2003) 395–406.
- [13] M.J. Carney, N.J. Robertson, J.A. Halfen, L.N. Zakharov, A.L. Rheingold, Organometallics 23 (2004) 6184–6190.
- [14] B.L. Small, M.J. Carney, D.M. Holman, C.E. O'Rourke, J.A. Halfen, Macromolecules 37 (2004) 4375–4386.
- [15] A.K. Tomov, J.J. Chirinos, D.J. Jones, R.J. Long, V.C. Gibson, J. Am. Chem. Soc. 127 (2005) 10166–10167.
- [16] W. Zhang, W.-H. Sun, S. Zhang, J. Hou, K. Wedeking, S. Schultz, R. Fröhlich, H. Song, Organometallics 25 (2006) 1961–1969.
- [17] L. Xiao, M. Zhang, W.-H. Sun, Polyhedron 29 (2010) 142–147.
- [18] D. Gong, X. Jia, B. Wang, X. Zhang, L. Jiang, J. Organomet. Chem. 702 (2012) 10–18.
- [19] S. Trofimenko, Chem. Rev. 93 (1993) 943–980.
- [20] H.R. Bigmore, S.C. Lawrence, P. Mountford, C.S. Tredget, Dalton Trans. (2005) 635–651.
- [21] C. Pettinari, R. Pettinari, Coord. Chem. Rev. 249 (2005) 525–543.
- [22] D.P. Long, P.A. Bianconi, J. Am. Chem. Soc. 118 (1996) 12453–12454.
- [23] S. Murtuza, O.L. Casagrande, R.F. Jordan, Organometallics 21 (2002) 1882–1890.

- [24] K. Michiue, R.F. Jordan, *Macromolecules* 36 (2003) 9707–9709.
- [25] K. Michiue, R.F. Jordan, *Organometallics* 23 (2004) 460–470.
- [26] J.T. Dixon, M.J. Green, F.M. Hess, D.H. Morgan, *J. Organomet. Chem.* 689 (2004) 3641–3668.
- [27] R. Rojas, M. Valderrama, G. Wu, *Inorg. Chem. Commun.* 7 (2004) 1295–1297.
- [28] I. García-Orozco, R. Quijada, K. Vera, M. Valderrama, *J. Mol. Catal. A: Chem.* 260 (2006) 70–76.
- [29] K. Michiue, R.F. Jordan, *J. Mol. Catal. A: Chem.* 282 (2008) 107–116.
- [30] J. Zhang, A. Li, T.S.A. Hor, *Organometallics* 28 (2009) 2935–2937.
- [31] J. Zhang, A. Li, T.S.A. Hor, *Dalton Trans.* (2009) 9327–9333.
- [32] D. Zabel, A. Schubert, G. Wolmershäuser, R.L. Jones, W.R. Thiel, *Eur. J. Inorg. Chem.* (2008) 3648–3654.
- [33] D.L. Reger, R.F. Semeniuc, M.D. Smith, *Cryst. Growth Des.* 5 (2005) 1181–1190.
- [34] A.R. Karam, E.L. Catarí, F. López-Linares, G. Agrifoglio, C.L. Albano, A. Díaz-Barrios, T.E. Lehmann, S.V. Pekerar, L.A. Albornoz, R. Atencio, T. González, H.B. Ortega, P. Joskowics, *Appl. Catal. A* 280 (2005) 165–173.
- [35] H. Abbo, S.J. Titinchi, *Catal. Lett.* 139 (2010) 90–96.
- [36] R. Gupta, R. Mukherjee, *Polyhedron* 20 (2001) 2545–2549.
- [37] A.K. Sharma, A. De, V. Balamurugan, R. Mukherjee, *Inorg. Chim. Acta* 372 (2011) 327–332.
- [38] K.-s. Son, J.O. Woo, D. Kim, S.K. Kang, *Acta Crystallographica Section E* 70 (2014) o973.
- [39] K.-s. Son, J.O. Woo, D. Kim, S.K. Kang, *Acta Crystallographica Section E* 71 (2015) m75–m76.
- [40] C.L. Foster, C.A. Kilner, M. Thornton-Pett, M.A. Halcrow, *Polyhedron* 21 (2002) 1031–1041.
- [41] J. Hurtado, D.M.-L. Carey, A. Muñoz-Castro, R. Arratia-Pérez, R. Quijada, G. Wu, R. Rojas, M. Valderrama, *J. Organomet. Chem.* 694 (2009) 2636–2641.